Countercurrent Gas-Liquid Annular Flow, Including the Flooding State

The structure of the wavy interface on a falling liquid film is studied for conditions of countercurrent gas flow in order to investigate mechanisms for flooding. Measurements taken just below the liquid feed and at 1.7 m down the tube show that under all conditions, including flooding, the waves propagate only downward and are never of such amplitude as to bridge the tube. These observations are in contrast to speculations in the literature that upward flow of waves or bridging of liquid due to waves cause flooding. In the mechanism suggested, flooding is due to flow reversal in the film just at the liquid entry.

G. J. Zabaras, A. E. Dukler
Department of Chemical Engineering
University of Houston
Houston, TX 77004

Introduction

The interaction between a falling liquid film and a countercurrent gas stream has been the subject of numerous investigations over the past forty years. The main difficulty in understanding this interaction is the presence of waves on the falling liquid film. As the counterflow gas rate is increased a critical value is eventually reached at which upward flow of some liquid is observed. Different investigators have reported that this condition of flooding is accompanied by a variety of phenomena including: a sharp increase in pressure gradient, entrainment of liquid in the gas in the form of drops, and the appearance of enhanced chaotic wave motion at the interface. As the gas rate is increased the liquid rate flowing down is known to decrease until all of the liquid flows upward.

Suitable models for the onset of flooding are lacking because the mechanism is not yet understood. But the practical importance of being able to predict this condition is evident from the variety of situations where flooding can cause deleterious effects. This includes emergency cooling systems in nuclear reactors, vertical countercurrent condensers, and gas-liquid reactors, among many possible examples.

A series of experimental studies has produced a number of empirical correlations, including those of Wallis (1969), Pushkina and Sorokin (1969), Kamei et al. (1954), Feind (1960), Tobilevich et al. (1968), Bharathan et al. (1978, 1979). However, a satisfactory law applicable over a wide range of fluid properties and tube sizes is still lacking because these correlations do not rest in physical understanding of the mechanisms that control the process.

Correspondence concerning this paper should be addressed to A. E. Dukler. G. J. Zabaras is currently with Shell Development Co., Houston, TX.

Other investigators of this problem have suggested some simple mechanisms for flooding as a basis for arriving at predictive equations. These have been categorized by Maron and Dukler (1984). Richter (1981), Taitel et al. (1982), and Maron and Dukler advance mechanisms determined only by the velocity distributions created in the films as if the gas liquid interface were smooth. Maron and Dukler also develop a model based on entrainment and a model using the existence of a flow-limiting kinematic wave in the liquid. The large number of remaining models can be categorized as being based on the existence of interfacial waves in one way or another.

Various ways in which waves can cause flooding have been suggested. Two of these are:

1. At flooding the waves become unstable; they grow explosively and either tend to block the gas flow, thus causing the liquid to be forced up as intermittent liquid slugs, or are broken up by the fast-moving gas and flow upward as liquid entrainment. The flooding point is then the condition at the onset of instability, and the model to find the flow rates at flooding is equivalent to that for finding the condition for instability of the interfacial waves. Good expositions of these ideas can be found in papers by Imura et al. (1977) and Zvirin et al. (1978).

2. At gas rates below flooding the waves are seen to flow downward on the interface. With increasing gas flow, as the flooding point is approached the wave velocity decreases until at flooding it is stationary. Then an incremental increase in gas rate causes the waves to flow upward, carrying liquid, and thus flow reversal takes place. These ideas underlie the papers by Shearer and Davidson (1965), Cetinbudaklar and Jameson (1969), and most recently by McQuillan et al. (1985). In the latter study the authors report observing momentary stationary waves followed by upward wave flow as the pressure is suddenly reduced to induce flooding.

Unfortunately none of these models—those based on film flow, entrainment, kinematic wave, or interfacial wave mechanisms—appears to produce results that are in general agreement with data over any significant range of operating conditions. Therefore a study was undertaken to develop an increased understanding of the mechanisms controlling gas-liquid interactions in countercurrent flow including conditions of flooding. In this paper we report the results of measurements of the distribution of liquid between upflow and downflow along with the time-varying measurements of local film thickness, wall shear stress, and pressure gradient. It will be shown that these measurements make it possible to evaluate a number of physical mechanisms underlying models that have been proposed for flooding and will show them to be inaccurate. The data presented lead to new qualitative conclusions regarding the flooding mechanisms. Modeling studies of the wavy interface are reported in a separate paper (Brauner et al., 1987).

Experimental Equipment and Measuring System

The two test sections used in this work are shown schematically in Figure 1. The measured quantities are local instantaneous values of liquid film thickness, wall shear stress, and pressure gradient. In configuration A the distance between the bottom of the inlet sinter to the measuring location was 0.15 m and in configuration B, 1.7 m. The liquid feed entered the column through a stainless steel porous sinter having 100 μm pore size. The probe station consisted of a 290 mm long section of 50.8 mm dia. Plexiglas piping matched to the inside diameter of the main test section. Mounted in this measuring section were two sets of parallel wire conductance probes, a double wall shear stress probe, and a differential pressure transducer reading the difference over 89 mm. An electrochemical method was used as a transducer for wall shear stress and a variable reluctance transducer used for the pressure measurement. The measuring section could be removed easily from the test section for calibration.

The liquid used was a 1.0 M solution of NaOH into which was dissolved 0.005 M each of potassium ferrocyanide and ferricyanide. Data were collected for four liquid feed rates as listed below, each over a range of counterflow gas rates to carry the system through flooding to the point of zero liquid downflow.

W_F, kg/s	0.0126	0.0315	0.0635	0.126
Re_F	310	768	1550	3100

where W_F is the mass feed rate and Re_F is the film Reynolds number Analog data from the transducers was digitized at 500 Hz and at least 2 min. of record was stored for subsequent processing. Air rates ranged from 0 to 0.0355 kg/s or a maximum Re_G of about 45,000. All measurements were carried out at near atmospheric pressure and temperature.

Details of individual measuring systems, units of equipment, electronic instrumentation, test procedures, error estimates, and software are given by Zabaras (1985) where complete tabulations of experimental data also appear.

Measurements

Flooding curve

Downflow liquid rates were measured for two test section configurations somewhat different from those used to make the local measurements; these appear in Figure 2. Consistent with many similar observations in the past, the experimental flooding curve is independent of liquid feed rate. That is, the gas rate at which flooding will be observed at a low liquid feed rate, say 0.031 kg/s, will be identical to the gas rate at which, for a higher liquid feed rate, say 0.126 kg/s the downward flow rate of liquid is also 0.031 kg/s. As will be shown below, similar identities exist for all measureable characteristics of the film, including

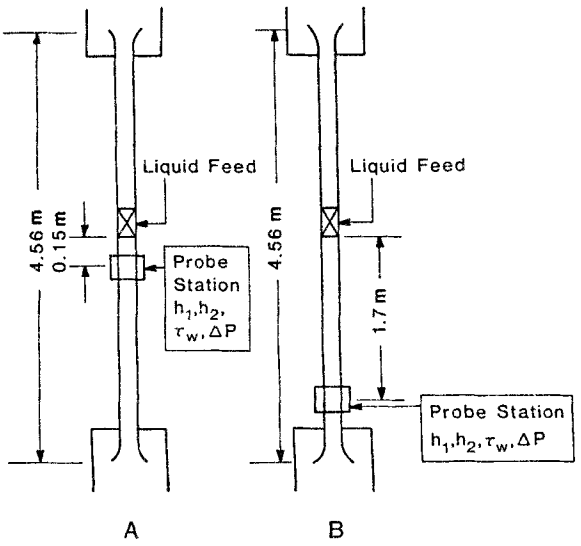

Figure 1. Test sections: I.D. = 50.8 mm.

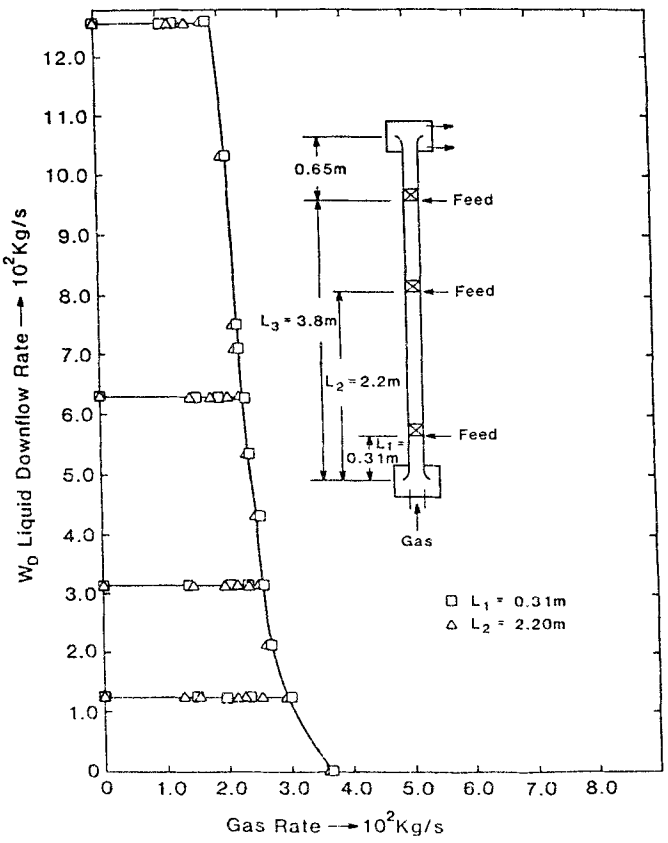

Figure 2. Liquid downward film flow rate.

mean and maximum film thickness, wave amplitude, and wall shear stress. This observation implies that the condition of onset or transition to flooding for any liquid feed rate is no different than the steady state operation of the liquid film in countercurrent flow.

It is clear that the flooding curve is independent of the test section length over this range of lengths, although data not shown here indicated that there was a small influence of length when the section was about 4 m long. Evidently, the effect of length on the flooding curve is not as profound here as in the studies by Hewitt et al. (1965) and by Whalley and McQuillin (1983). The reason continues to be elusive.

Film thickness data and analysis

The mean film thickness calculated as a time average over 120 s of data is shown in Figure 3 for both test section configurations shown in Figure 1. The broken lines are the Nusselt film thicknesses that correspond to laminar flow in the absence of interfacial waves and counterflow of gas. Increasing the gas rate at any liquid rate results in an increase in the mean film thickness, with the effect accelerating as the flooding condition is approached. However, it is equally clear that flooding is not necessarily the condition at which a very drastic increase in film thickness suddenly takes place. In fact, when the data points happen to be fortuitously spaced it is possible to show that the process of reaching flooding may not be nearly as precipitous as indicated by earlier studies in which data points were not so closely taken. The process may be described as one in which the mean film thickness increases in a monotonic way with gas flow, the dependency being exponential.

This observation is reinforced by the data that appear in Figure 4. A film thickness tracing program was written to extract

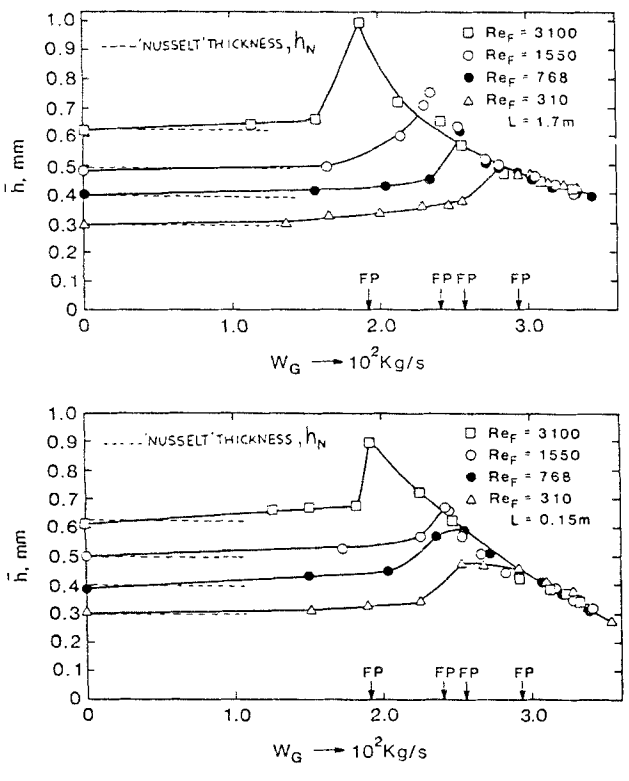

Figure 3. Mean film thickness.

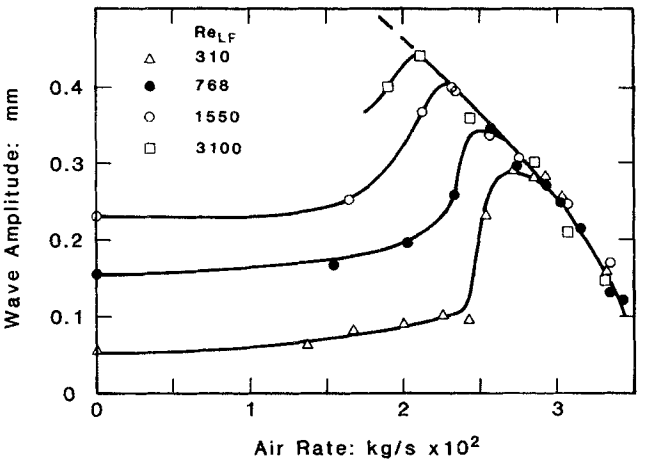

Figure 4. Average amplitude values.

information on wave amplitude from the time traces of the film thickness. A change in film thickness was categorized as a large wave when a minimum was detected at a film thickness below the mean and a maximum located above the mean film thickness was observed following this minimum. The 120 s of film thickness record for each run was analyzed in this way to calculate average properties of the waves. Average amplitude values appear in Figure 4. Each point represents the average of over 2,000 waves. Small waves existed on the substrate whose minimum and maximum both occurred below the mean film thickness. However these small capillary waves were not included in the computations.

For the location $L = 1.7$ m the results can be interpreted as a process where the wave amplitude depends on the gas rate exponentially rather than where the wave amplitude changes drastically just at the flooding point. In fact for each liquid rate there are observed runs where the wave amplitude was substantially elevated and flooding had not yet taken place. However the observations are quite different for configuration A, where the feed was introduced only 0.15 m above the measuring station. Here the surface was smooth or covered by small capillary waves at conditions below flooding. As gas rates were raised to near flooding there was a much more precipitous increase in wave amplitude, followed by decreased amplitude with increasing gas rate along a flooding curve similar to that seen in Figure 4. Thus, well below the feed location the liquid seems to behave as a wavy falling film subject to countershear but is in no way unique because it is observed along the flooding curve. However at the entry region, the film appears to change suddenly at the flooding conditions.

Of particular importance is information about the maximum film thickness. Figure 5 shows the maximum film thickness values for data taken at $L = 1.7$ m, calculated as the average of the 10 largest values detected during each 120 s run, during which time over 2,000 large waves were observed. Despite suggestions that bridging occurs during flooding as discussed above, the maximum film thickness never exceeded 20% of the pipe radius. Data taken at 0.15 m below the feed (configuration A) show an identical result. It thus seems safe to conclude that *flooding models based on wave growth followed by bridging of the pipe by liquid are not supported by the facts.*

Figure 6 shows typical normalized cross-covariance traces calculated from film thickness signals taken from two transduc-

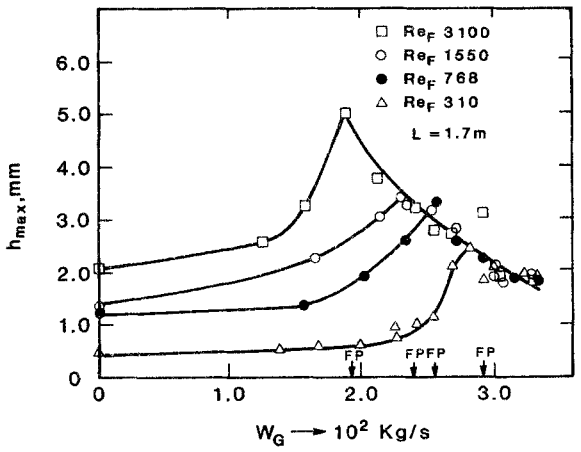

Figure 5. Maximum film thickness at L = 1.7 m.

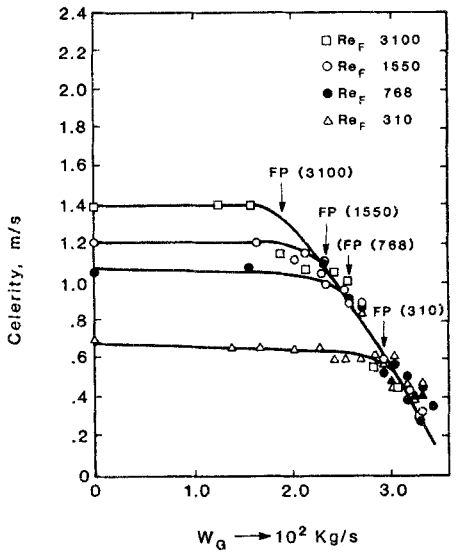

Figure 7. Wave velocity at L = 1.7 m.

ers located 53 mm apart. Data collected at gas rates below, just at, and above flooding are shown for one liquid rate. The curves all display a characteristic well-defined peak at a measurable time delay, which makes possible calculating the wave velocity once the distance between transducers is known. The direction is indicated by the sign of the time delay, and in every case measured the velocity was downward-directed. Wave velocities determined in this way are shown in Figures 7 and 8 for the two configurations. The waves at the 0.15 m location were less well defined, especially at low gas rates well below flooding, and thus the celerities were more difficult to obtain accurately. However, it is quite clear that all along the flooding curve the waves travel downward and under no circumstances do they reverse. In fact, for configuration B it appears that the wave velocity is quite insensitive to increases in gas rate until just at the flooding point. Then the decrease in wave velocity is associated with the decrease that takes place in liquid flow rate along the flooding curve. Early studies by Hewitt and Wallis (1963) indicated that there was no marked effect on wave velocity of counterflow rate of gas below flooding. These new data extend that conclusion to the flooding point itself.

In the light of this conclusion, there remains the problem of explaining the recent results of McQuillan et al. (1985). Their experiments were carried out by bringing the system to just below flooding, equilibrating to steady state, and then suddenly dropping the pressure a small amount to induce a sharp increase in gas velocity. Photographic observations were made for a few tenths of a second. It is suggested that the upflow was associated with a short transient required to adjust the liquid inventory to its value under the new gas velocity. Had the observations been continued, the downward motion of the waves would have resumed. It thus becomes important to discriminate between flooding mechanisms associated with fast transients and those associated with slower flooding conditions. Perhaps this difference can explain the wide disparity of the data in the literature. *Models based on the idea that waves reverse direction at flooding and flow upward are not supported by the facts.*

Wall shear stress

The time-averaged wall shear stress as measured by electrochemical wall probes is plotted in Figure 9. In these experiments the use of double probes showed that *in all instances of countercurrent flow, including conditions along the flooding curve, the*

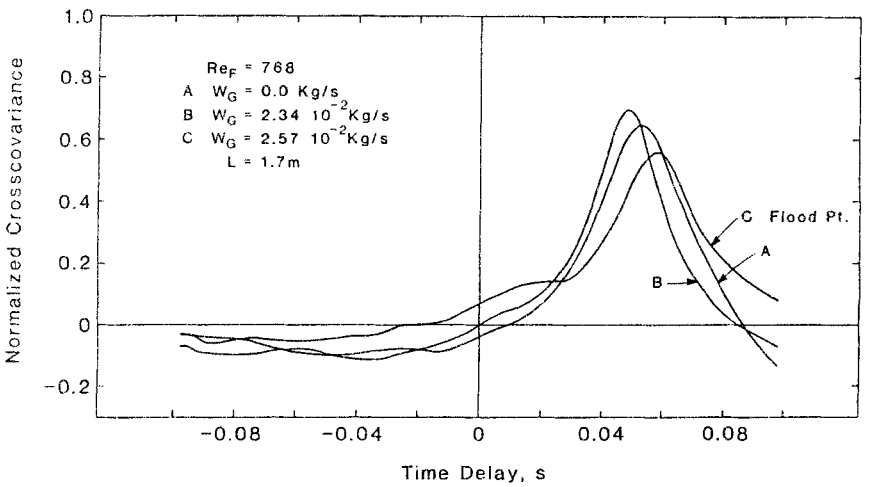

Figure 6. Normalized cross covariance for two film thickness signals: Re_F = 768 and L = 1.7 m.

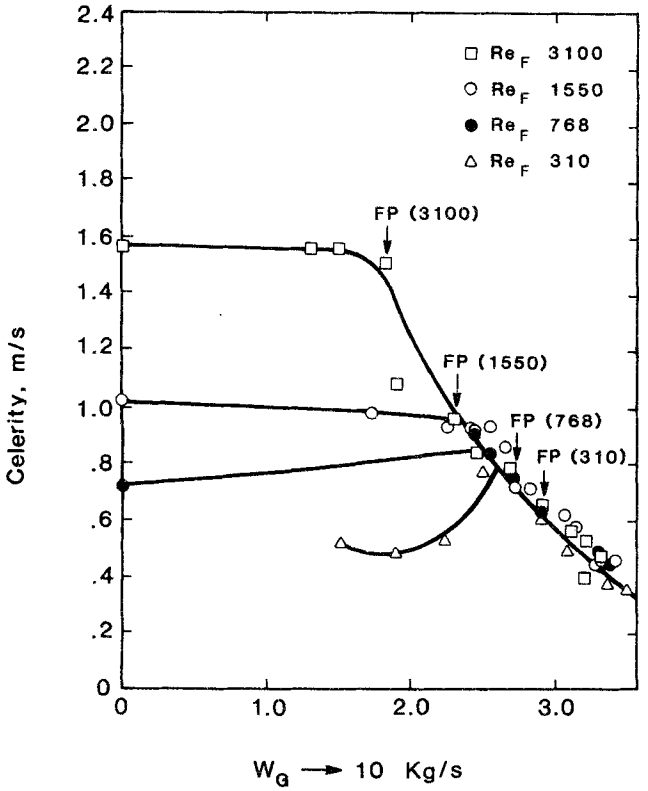

Figure 8. Wave velocity at L = 0.15 m.

wall shear was directed upward and thus the velocity near the wall was directed downward.

The broken lines in Figure 9 represent the wall stress computed from the parabolic distributions of the Nusselt equations. The good agreement at zero gas rate appears to validate the

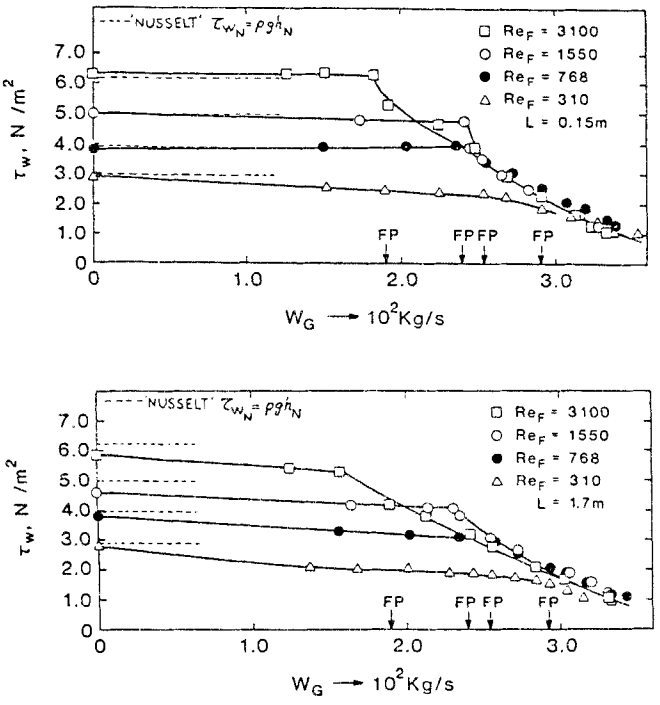

Figure 9. Mean wall shear stress.

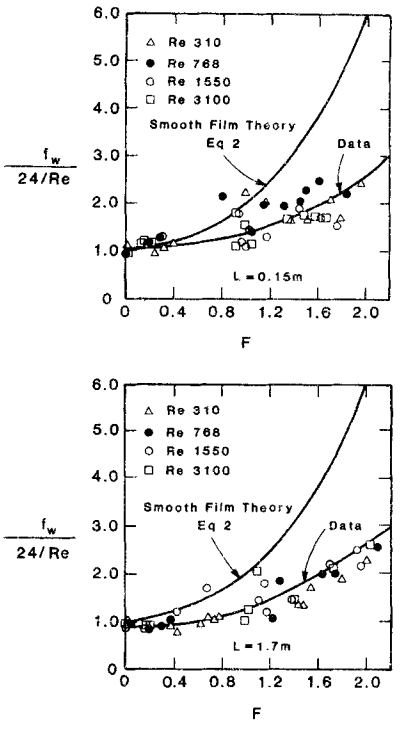

Figure 10. Wall friction factor.

measuring method. With increasing gas rate the wall shear decreases, as expected, since the interfacial shear now supports part of the force of gravity on the film. The wall shear stress can be generalized by its dimensionless form, the wall friction factor f_W:

$$f_W = 2\tau_W/\rho V_L^2 \tag{1}$$

where V_L is the mean liquid velocity in the film. With the measurements reported here (mean wall stress, film flow rate, mean film thickness) it is now possible to calculate f_W unambiguously. In the absence of interfacial shear and assuming a smooth laminar film without waves, $f_W = 24/Re$, where Re is calculated from the actual liquid rate flowing downward. Maron and Dukler (1984) extended this result to the case of counterflow of gas to yield:

$$f_W = (24/Re)\,\Psi \tag{2}$$

where

$$\Psi = (2 + F)/(2 + 1.5F)$$

$$F = 2\tau_i/\rho g h$$

Figure 10 shows experimental values of f_W normalized by $24/Re$ compared with Eq. 2. At low values of interfacial shear, experimental friction factors are in good agreement with $24/Re$ even for Reynolds numbers as high as 3,100. This reinforces the idea that in wavy films the flow may be laminar even at liquid rates where the film has been considered turbulent, as discussed by Maron et al. (1985). At higher counterflow gas rates the wall friction factor increasingly deviates from the theory. Since Eq. 2 is based on the premise of a smooth film, this result is not

surprising. Models of the interfacial wave structure in the presence of interfacial shear (Maron et al., 1987) show that a substantial portion of the liquid in a wave exists in a region of negligible velocity gradient. In addition, the shear stress in the thin substrate separating the larger waves results in low values of wall shear. Prediction of average values of the wall friction factor must turn to waveform analysis methods. However, the use of a constant value such as $f_W = 0.005$, which is commonly seen in the literature and in computer programs, is clearly in error.

Interfacial shear stress

Interfacial shear stress was calculated from the measured mean pressure gradient and film thickness values. These were used to compute an interfacial friction factor neglecting the unknown interfacial velocity in calculating the kinetic energy of the gas relative to the interface. The values of f_i plotted as a function of h/D, the mean film thickness to tube diameter as originally suggested by Wallis (1969), appear in Figure 11. Shown by comparison is the correlation suggested by Bharathan et al. (1978). That this correlation is in reasonable agreement with the data is not surprising in view of the fact that it was

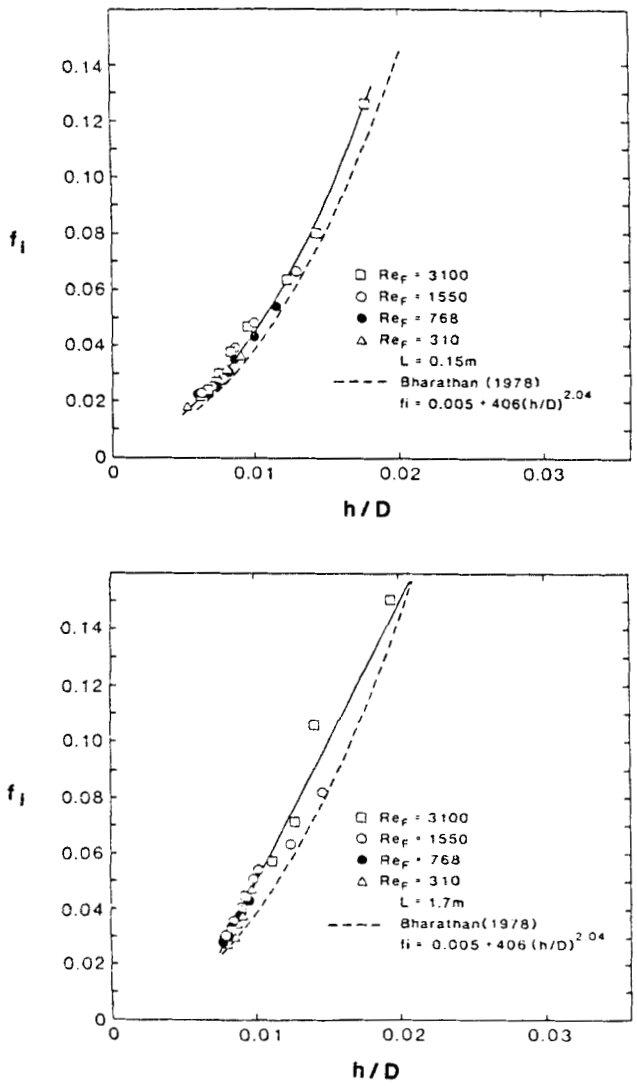

Figure 11. Interfacial friction factor.

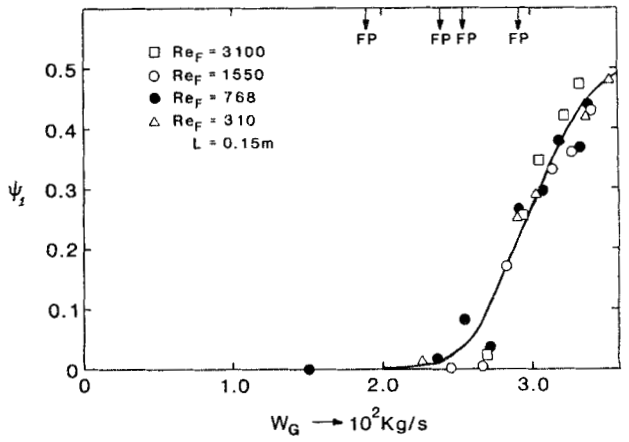

Figure 12. Fraction of time for upflow in the film at L = 0.15 m.

based largely on data taken under similar conditions as the data shown here. The recent correlation suggested by Asali et al. (1986) for upward and downward cocurrent flow was tested against the data, yielding values that were only about one-third the experimental values.

Flow in the Wave along the Flooding Curve

A detailed study of the flow along the wavy interfaces reveals some surprises. Data presented above demonstrate that the velocity of waves on the interface is directed downward for all conditions below the feed, including along the flooding curve. The integral material balance can now be applied to any position along the wavy surface to obtain the following:

$$h(V_W - V) = \gamma \tag{3}$$

where V is the average liquid velocity at a local position along the wave having a thickness of h, V_W is the wave velocity, and γ is the volumetric rate at which slow-moving fluid in front of a wave is picked up (per unit perimeter) when observed in a coordinate system moving with the wave. γ must be a constant for any downward liquid flow rate at all points along a wave, as can

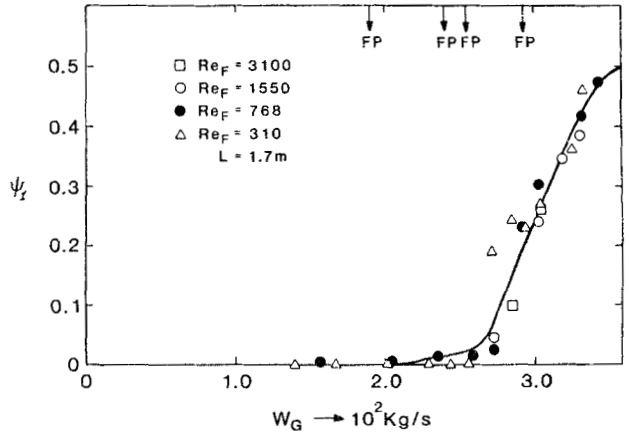

Figure 13. Fraction of time for upflow in the film at L = 1.7 m.

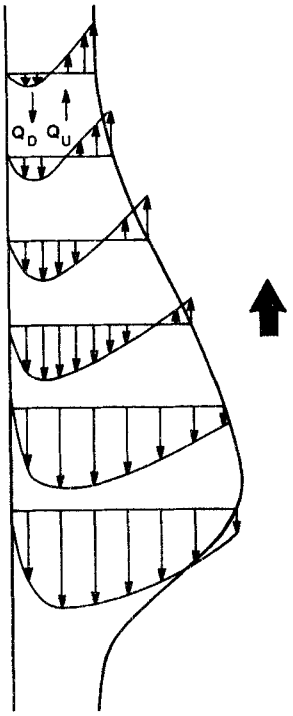

Figure 14. Time trace of the film thickness voltage signal.

be seen by integrating Eq. 3 over a wavelength:

$$\gamma = \langle h \rangle V_W - \Gamma/\rho \tag{4}$$

where Γ is the downward liquid mass film flow rate per unit perimeter and $\langle h \rangle$ is the time-averaged film thickness. Rearranging Eq. 3 gives

$$V = V_W - \gamma/h \tag{5}$$

where V is positive when downward-directed. Equation 5 can be used to obtain information on the variation in mean velocity and its direction along the wave as h varies. At any local position along the wave having a thickness h, $V < 0$ indicates that the mean flow at that cross section is upward. Note that these negative values of V can be expected to exist for the smallest values of h, *thus upflow will take place in the substrate region, if it takes place at all.*

For each experimental run measured values of $\langle h \rangle$, V_W, and Γ were used to compute γ. The digital film thickness records were then searched to determine those portions of the trace that indicated the existence of a negative (upward) mean velocity. The results expressed in fraction of time during which the net flow is upward, ψ_1, are shown in Figures 12 and 13. With free-falling liquid films in the absence of counter gas flow, upward flow in the film was never observed for any liquid flow rate. However at a gas rate of approximately 0.02 kg/s of air flow, upflow starts in the substrate, approaching a value of 0.5 at the "hanging film" condition where downflow can no longer be observed. As discussed above, measurements showed that the wall shear was directed upward without exception in all of these runs. Therefore it is clear that the interfacial shear causes a reversal in the velocity distribution in that substrate region, as shown in Figure 14, and this suggests that a portion of the flow must be directed upward at thicker portions of the wave. At distances well below the entry this will simply result in mixing with the wave above. However, in the entry region this delivery of liquid above the feed can be a mechanism for flooding itself.

An experiment that reveals some other features of flooding is one in which the feed rate undergoes a large step change. With the probe station located 0.15 m below the inlet sinter, the liquid feed rate was changed by a factor of 10 in a step from $Re_F = 310$ to 3,100. The change was made in less than 0.2 s. A time trace of film thickness which was started before the step and continued afterward is shown in Figure 15. What is quite evident is that there is no observable effect of this tenfold change in feed rate on the film structure at a location only 15 cm below the feed. The implication is clear: the split between up and downflow *takes place at the feed location.* The conditions below the feed, such as wave velocity or interfacial shear stress, seem to play no role in determining the condition for flooding.

Additional Speculations on Mechanism

The various observations presented above present a somewhat different picture than drawn previously. We now speculate that the process of flooding is controlled by conditions that exist at or close to the point of feed entry. That is, the split in flow between up and down is controlled by the mechanics of the flow at or just below the feed. What is observed at distances well below this point is simply the result of counterflow of gas against a falling liquid film and is not in any way related to the flooding state. Conditions that are created by countershear at flooding create large waves at the feed location within which there are flow reversals. In this way liquid is delivered above the feed location, at which point the dynamics of cocurrent flow begin to control the process.

Experiments have been reported that run counter to this entry region controlling mechanism. These include tests that show a strong influence on flooding by the design of the liquid discharge piping at the bottom of the tube (cutoff angle), those that show an effect of tube length below the feed on the flood point, and observations which suggest that flooding starts at the bottom of the tube. Each of these can be explained, although additional work will be needed to tie down the matter.

As to the effect of tube length, longer tubes for the same gas

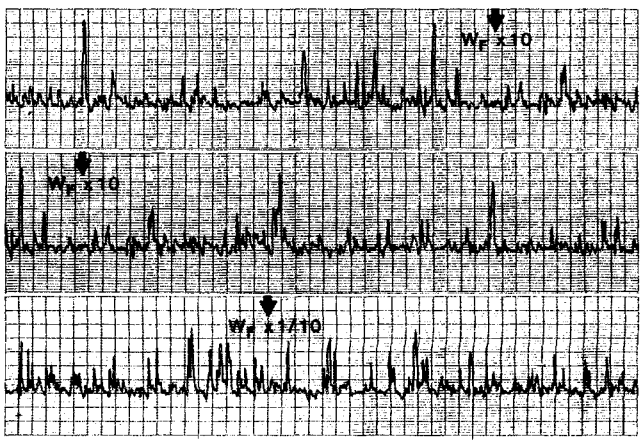

Figure 15. Velocity distribution with countercurrent gas flow.

mass flow rate may result in somewhat different gas densities at the entry location. A change in flood point can be a manifestation of the change in local velocity for the same gas rate as the tube length is changed. Flooding condition is very sensitive to this velocity.

The observation that flooding takes place at the bottom of the tube is, we believe, the result of the onset of flooding, a transient phenomenon. Once flooding has been achieved and the flow rate of gas is increased, flooding continues at decreasing liquid rates. Along the flooding curve there is no appearance of flooding at the bottom in preference to any other position.

The unquestioned fact that the onset of flooding takes place at different gas rates when the bottom of the pipe is tapered is more difficult to explain. We can only conjecture at this point that this might change the turbulence in the gas phase or the pressure drop so that at the liquid entry the velocity or the turbulence level in the gas differs. Further investigation is needed.

Acknowledgment

This work was made possible by the support of the National Science Foundation and the Shell Companies Foundation.

Literature Cited

Asali, J. C., T. J. Hanratty, and P. Andreussi, "Interfacial Drag and Film Height for Vertical Annular Flow," *AIChE J.*, **31,** 895 (1985).

Bharathan, D., G. B. Wallis, and J. J. Richter, "Air-Water Countercurrent Annular Flow in Vertical Tubes," EPRI NP-786 (1978).

———, "Air-Water Countercurrent Annular Flow," EPRI NP-1165 (1979).

Brauner, N., D. M. Maron, G. Zabara, and N. E. Dukler, "Interfacial Structure of Thin Falling Films: Piecewise Modeling of the Waves with Counter Shear," *Chem. Eng. Commun.*, **58,** 245 (1987).

Cetinbudaklar, A. G., and G. J. Jameson, "The Mechanism of Flooding in Vertical Countercurrent Two-Phase Flow," *Chem. Eng. Sci.*, **24,** 1669 (1969).

Feind, F., "Falling Liquid Films with Countercurrent Air Flow in Vertical Tubes," *VDI-Forschungsheft*, **481,** 26(1960).

Hewitt, G. F., and G. B. Wallis, "Flooding and Associated Phenomena in Falling Film Flow in a Tube," UKAERE Rept. R-4022 (1963).

Hewitt, G. F., P. M. C. Lacey, and B. Nicholls, "Transition in Film Flow in a Vertical Tube," *Proc. Two-Phase Flow Conf.*, Exeter, England (1965).

Imura, H., H. Kusuda, and S. Funatsu, "Flooding Velocity in a Countercurrent Annular Two-Phase Flow," *Chem. Eng. Sci.*, **32,** 79 (1977).

Kamei, S., J. Oishi, and T. Okase, "Flooding in a Wetted Wall Tower," *Chem. Eng. (Japan)*, **18,** 364 (1954).

Maron, D., and A. E. Dukler, "Flooding and Upward Film Flow in Vertical Tubes. II: Speculations on Film Flow Mechanisms," *Int. J. Multiph. Flow*, **10,** 599 (1984).

Maron, D., N. Brauner, and A. E. Dukler, "Interfacial Structure of Thin Falling Films: Piecewise Modeling of the Waves" *Physiochem. Hydrodynam.*, **6,** 87 (1985).

McQuillan, K. W., P. B. Whalley, and G. F. Hewitt, "Flooding in Vertical Two-Phase Flow," *Int. J. Multiph. Flow*, **11,** 746 (1985).

Pushkina, O. L., and Y. L. Sorokin, "Breakdown of Liquid Film Motion in Vertical Tubes," *Heat Trans.-Soviet Res.*, **1,** 56 (1969).

Richter, H. J., "Flooding in Tubes and Annuli," *Int. J. Multiph. Flow*, **7,** 647 (1981).

Shearer, C. J., and J. F. Davidson, "The Investigation of a Standing Wave Due to Gas Blowing Upwards Over a Liquid Film; Its Relation to Flooding in Wetted-Wall Columns," *J. Fluid Mech.*, **22,** 321 (1965).

Taitel, Y., D. Barnea, and A. E. Dukler, "A Film Model for Flow Reversal and Flooding," *Int. J. Multiph. Flow*, **8,** 1 (1982).

Tobilevich, N. Y., I. J. Sagan, and Y. G. Porzhezihskii, "The Downward Motion of a Liquid Film in Vertical Tubes in an Air-Vapor Counter Flow," *J. Eng. Phys.*, **15,** 10711 (1968).

Whalley, P. B., and K. W. McQuillan, "Flooding in Two-Phase Flow: The Effect of Tube Length and Artificial Wave Injection," AERE-R 10883 rep. (1983).

Zvirin, Y., R. B. Duffey, and K. H. Sun, "On the Derivation of a Countercurrent Flooding Theory," *Symp. Fluid Flow, Heat Transf. Over Rod or Tube Bundles*, ASME, New York, 111 (1978).

Zabaras, G. J., "Studies of Vertical Annular Gas-Liquid Flows," Ph.D Thesis, Univ. Houston, TX (1985).

Manuscript received Jul. 22, 1987, and revision received Oct. 12, 1987.